Biointerface Research in Applied Chemistry
Open-Access Journal (ISSN: 2069-5837)

Article
Volume 16, Issue 3, 2026, 82
https://doi.org/10.33263/BRIAC163.082

Molecular-docking of some Amines and Furane Derivatives with IRAK-4 Using a Theoretical Model

Rosas-Nexticapa Marcela [1,*], Alvarez-Ramirez Maria Magdalena [1], Bonilla-Zavaleta Enrique [1], Melgarejo-Gutiérrez Montserrat Alheli [2], Ramírez-Higuera Abril [3]

[1] Nutrition Laboratory, Faculty of Nutrition, University of Veracruz, Medicos y s/n Odontologos 910210, Unidad del Bosque, Xalapa, Mexico
[2] Faculty of Medicine, University of Veracruz, Médicos y Odontologos s/n C.P. 91010, Unidad del Bosque, Xalapa, Mexico
[3] Institute of Basic Sciences. University of Veracruz. Av. Castelazo Ayala Sn, Industrial Ánimas, 91192 Xalapa-Enríquez, Veracruz, Mexico
* Correspondence: nmrosas@uve-mail.com;

Received: 29.01.2026; Accepted: 1.03.2026; Published: 15.06.2026

Abstract: For several years, some IRAK-4 inhibitors have been developed to treat chronic lymphocytic leukemia; however, their interaction with the IRAK-4 kinase is unclear. The aim of this study was to evaluate the interaction of some amine and furanone derivatives with IRAK-4 as a therapeutic alternative to treat chronic lymphocytic leukemia. The theoretical coupling of amine and furanone derivatives with the IRAK-4 was carried out using the 5uit protein as a theoretical model. Besides, 1-439 PF-3758309, 336113-53-2, 509093-47-4, ND-2158, and emavusertib drugs were used as controls in the DockingServer program. The results displayed different types of amino acid residues involved in the interaction of amine and furanone derivatives with the 5uit protein surface compared to the controls. Besides, the inhibition constant was lower for amino derivatives 3, 9, 25, 33, and 36 compared with the controls. Other data indicate that the inhibition constant was lower for furanone analogs 1, 3, 7, 13, 27, 32, and 34 compared with PF-3758309, 336113-53-2, 509093-47-4, ND-2158, and emavusertib. In conclusion, theoretical data indicate that amine (3, 9, 25, 33, and 36) and furanones (1, 3, 7, 13, 27, 32, and 34) derivatives might have a higher affinity for the 5uit protein surface compared with the controls. This data suggests that both amino and furanone derivatives can act as IRAK-4 inhibitors, which may serve to treat chronic lymphocytic leukemia.

Keywords: chronic lymphocytic leukemia; IRAK-4; theoretical model; amine; furanone.

1. Introduction

Chronic lymphocytic leukemia is a global health problem that reduces the quality of life of the population [1-3]. This clinical pathology is characterized by the expansion of monoclonal mature B lymphocytes expressing CD5 and CD23 in the blood, bone marrow (BM), lymph nodes, and spleen [4]. It is important to note that some studies have reported an association between factors involved in the inflammatory process and chronic lymphocytic leukemia, such as interleukins [5-7]. For example, interleukin-1 receptor-associated kinases (IRAK1, IRAK2, IRAK3, IRAK4) exert their activity through multiple inflammatory pathways involved in hematologic malignancies [8]. In this way, the study indicates that interleukin-1 receptor-associated kinase 4 (IRAK-4) may mediate the inflammatory process in chronic

lymphocytic leukemia [9]. Furthermore, a report suggests that IRAK-4 may play an important role in the development of acute myeloid leukemia [10, 11]. It is important to note that some IRAK-4 inhibitors have been used to treat chronic lymphocytic leukemia; for example, a report indicates that emavusertib is used to treat lymphoid and myeloid malignancies [12]. Other data indicate that administration of ABT-737 (IRAK1/4 inhibitor) or vincristine may reduce leukemia burden in mice and prolong survival [13]. Furthermore, a study showed that ABT-737 was co-encapsulated into polyethylene glycol nanoparticles to enhance therapy against acute lymphoblastic leukemia [14]. Other reports showed that the CA-4948 drug (an IRAK-4/FLT3 inhibitor) can produce biological activity on acute myeloid leukemia with wild-type and mutated FLT3 (FMS-like tyrosine kinase 3) using a murine model [15]. Another study shows that the CA-4948 drug has beneficial effects in patients with acute myeloid leukemia or myelodysplastic syndrome [16].

On the other hand, some theoretical methods have been used to develop new IRAK-4 inhibitors; for example, the synthesis of compounds BAY1834845 and BAY1830839 and their theoretical activity on IRAK4 using Glide Software [17]. Other studies showed that a 5-azaquinazoline derivative may act as an IRAK-4 inhibitor using the 7C2V protein as a theoretical tool in the AutoDock program [18]. Furthermore, a study shows the interaction of the CA-4948 drug with IRAK-4 using the 7c2v protein as a tool in a theoretical model [19]. These data indicate that several compounds have been developed as IRAK-4 antagonists; however, there remains a need to develop selective inhibitors for the treatment of cancer and various autoimmune diseases. For this reason, the aim of this study was to determine the interaction of several compounds (with amino and furan functional groups) with IRAK-4 as a therapeutic alternative for the treatment of chronic lymphocytic leukemia.

2. Materials and Methods

Amino (Figure 1, Table 1) and furanone (Figure 2, Table 2) analogs were used to determine the interaction with the IRAK-4 surface as follows:

Table 1. Name of amino derivatives (1-43).

1) 3-(1H-indazol-5-yl)-N-propylimidazo[1,2-b]pyridazin-6-amine
2) (+)-3,4-Dihydroxyphenylalanine
3) (2-Methylbutyl)amine
4) 1,3-benzothiazole-2,6-diamine
5) 1,4-Benzodioxan-6-amine
6) 1,5-Naphthyridin-3-amine
7) 1-(4-Bromophenyl)-4-phenyl-1H-pyrazol-5-amine
8) 1-(4-chlorobenzyl)-3-phenyl-1H-pyrazol-5-amine
9) 1-(4-Fluorophenyl)-4-phenyl-1H-pyrazol-5-amine
10) 1-Cyclopropyl-propylamine
11) 1-Phenyl-4-p-tolyl-1H-pyrazol-5-amine
12) 1-phenyl-N-(1-phenylethyl)ethanamine
13) 1H-Pyrrol-1-amine
14) 2,2',2"-Nitrilotriethylamine
15) 2-Cycloheptyl-ethylamine
16) 2-Cyclooctyl-ethylamine
17) 2-Cyclopropyl ethyl amine
18) 2-Ethyl-N,N-bis(2-ethylhexyl)hexan-1-amine
19) 2-Methoxy-N-(2-methoxyethyl)ethanamine
20) 2-Methylbut-3-yn-2-amine
21) 2-Phenyl-1,3-benzoxazol-5-amine
22) 2-Phenyl-1-benzofuran-5-amine
23) 3,5-Diiodo-pyridin-4-ylamine
24) 3-((2-Methylbenzyl)thio)-5-phenyl-4H-1,2,4-triazol-4-amine
25) 3-((4-Methoxybenzyl)thio)-5-phenyl-4H-1,2,4-triazol-4-amine
26) 3-(4-(Methylthio)phenyl)-1H-pyrazol-5-amine

27) 3-(Furan-2-yl)-1-phenyl-1H-pyrazol-5-amine
28) 3-Amino-1-(2-azatricyclo[10.4.0.0^{4,9}] he-xadeca-1(16),4,6,8,12,14-hexaen-10-yn-2-yl)propan-1-one
29) 3-Aminoimidazo[1,2-a]pyridine
30) 3-Buten-1-amine
31) 3-Butoxy-phenylamine
32) 3-Cyclopentyl-propylamine
33) 3-Methyl-pentylamine
34) 3-Phenyl-1H-indazol-5-amine
35) 3-tert-Butyl-1-phenyl-1H-pyrazol-5-amine
36) 4,5-Dimethoxypyridin-3-amine
37) 4,5-Dimethylisoxazol-3-amine
38) 4-(4-Bromophenyl)-1-phenyl-1H-pyrazol-5-amine
39) 4-(Ethylaminomethyl)pyridine
40) 4-Bromo-N-(4-bromophenyl)aniline
41) 4-Phenyl-1-p-tolyl-1H-pyrazol-5-amine
42) 4-Phenylisoxazol-5-amine
43) 5-(4-Trifluoromethyl-phenyl)-2H-pyrazol-3-ylamine

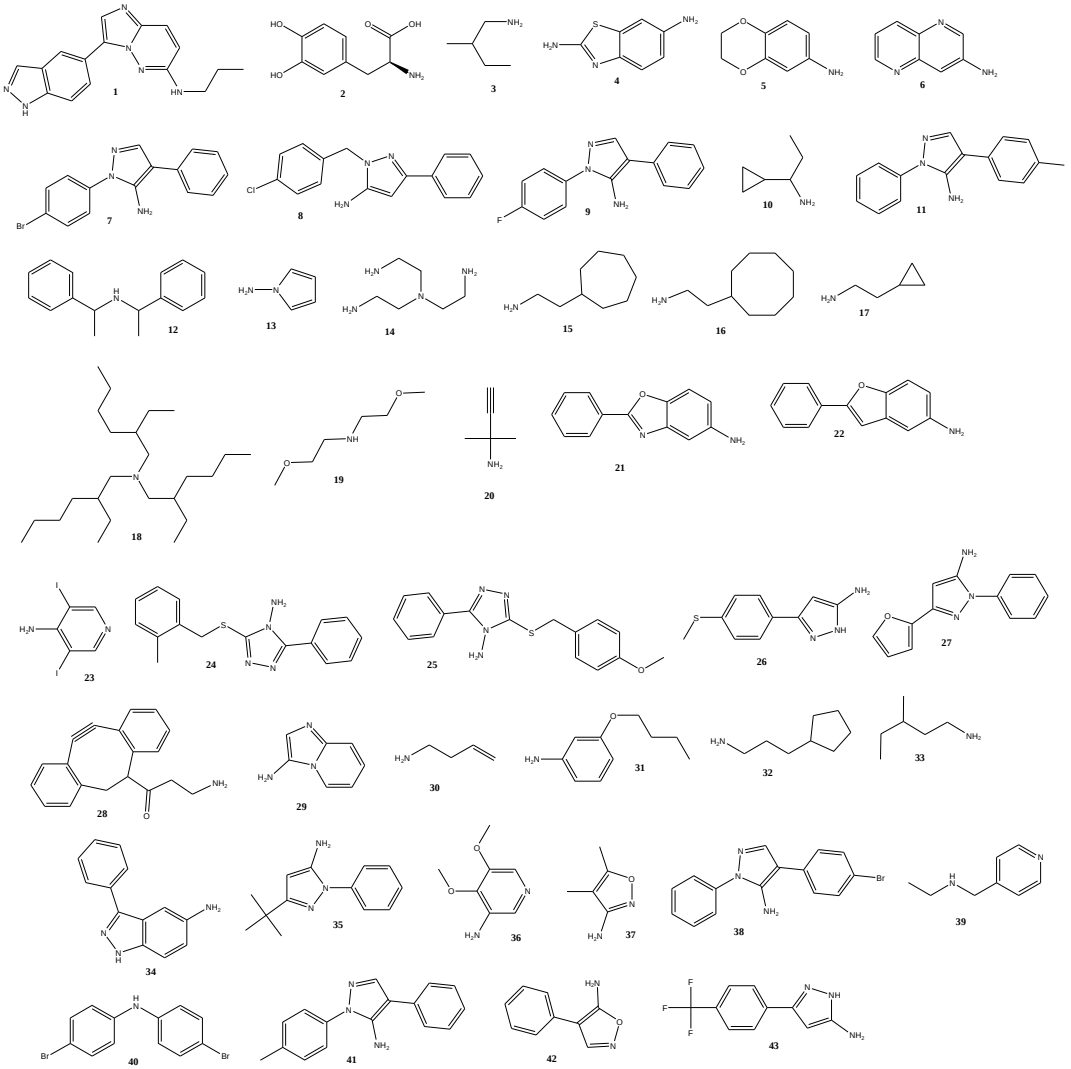

Figure 1. Chemical structure of amino derivatives (1-43). Source: https://pubchem.ncbi.nlm.nih.gov.

Table 2. Name of furanone analogs (1-35).

1) (4R)-4-Benzyl-3-(5-hexenoyl)dihydro-2(3H)-furanone
2) (5S)-5-{2-[(Benzyloxy)methoxy]ethyl}dihidro-2(3H)-furanone
3) (S)-(-)-5-Hydroxymethyl-2(5H)-furanone
4) (Z-)-4-Bromo-5-(bromomethylene)-2(5H)-furanone
5) 2,2-Dimethyl-5-phenyldihydro-3(2H)-furanone
6) 2,5-Dimethyl-3(2H)-furanone
7) 2,5-Dimethyl-4-methoxy-3(2H)-furanone
8) 2-Hydroxy-2,4,5-triphenyl-3(2H)-furanone
9) 2-Methoxy-2,4-diphenyl-3(2H)-furanone
10) 2-Methyltetrahydro-3-furanone

11) 3,3,5-Trimethyldihydro-2(3H)-furanone
12) 3,4,5-Triphenyl-2(3H)-furanone
13) 3,4-Dibromo-2(5H)-furanone
14) 3,4-Dichloro-2(5H)-furanone
15) 3,4-Dichloro-5-(oxo)-2-phenylethyl)-2(5H)-furanone
16) 3,4-Dichloro-5-(4-chlorophenyl)-5-hydroxy-2(5H)-furanone
17) 3-(Triphenylphosphoranylidene)dihydro-2(3H)-furanone
18) 3-Allyldihydro-2(3H)-furanone
19) 3-Bromo-5-(diphenylmethylene).2(5H)-furanone
20) 3-Methyl-2(5H)-furanone
21) 4-(2,2-Dichlorovinyl)-4,5-dihydro-5,5-dimethyl-2(3H)-furanone
22) 4-Acetoxy-2,5-dimethyl-3(2H)-furanone
23) 4-Anilino-2(5H)-furanone
24) 4-Bromo-5-(4-methoxy-phenyl)-3-methylamino-5H-furan-2-one
25) 4-Hydroxy-2,5-dimethyl-3(2H)-furanone
26) 4-Hydroxy-3-(1-(phenylimino)ethyl)-2(5H)-furanone
27) 4-Hydroxy-5-methyl-3-furanone
28) 4-Methoxy-2(5H)-furanone
29) 4-[(Cyclohexylamino)methyl]-3,3-diphenyldihydro-2(3H)-furanone
30) 5-(Chloromethyl)dihydro-2(3H)-furanone
31) 5-Ethyl-3-hydroxy-4-methyl-2(5H)-furanone
32) 5-Ethyl-4-hydroxy-2-methyl-3(2H)-furanone
33) Dihydro-2,2,5,5-tetramethyl-3(2H)-furanone
34) Dihydro-3-amino-2-(3H)-furanone
35) 5H-furan-2-one

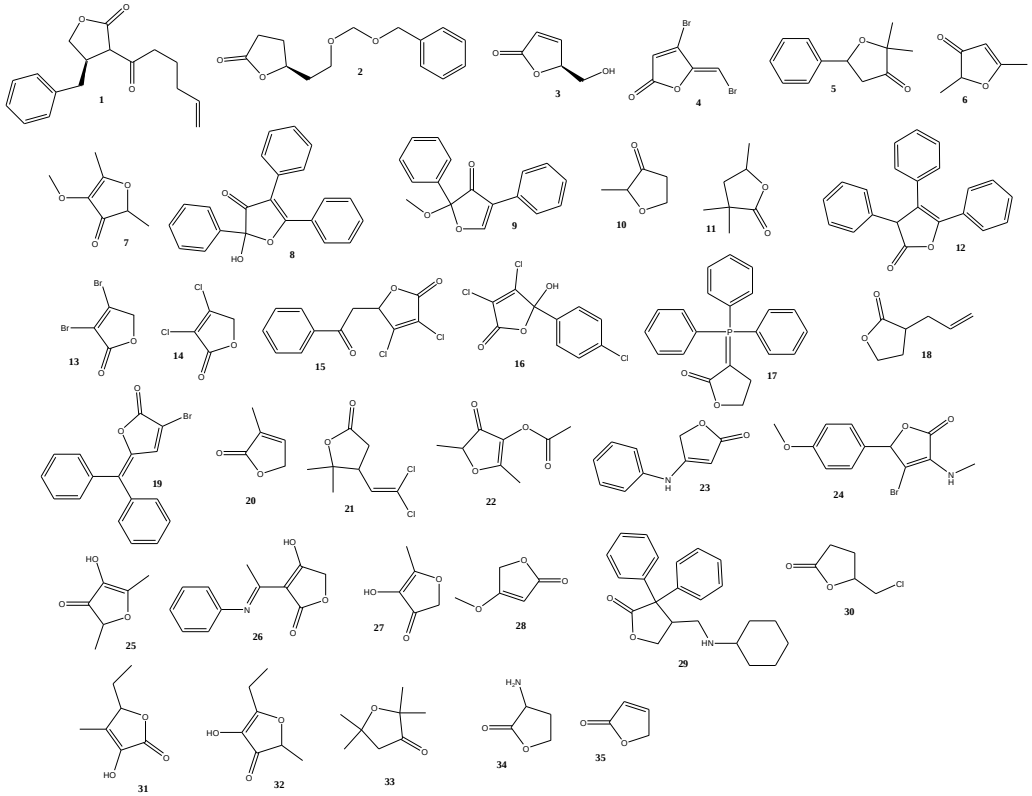

Figure 2. Chemical structure of furanone derivatives (1-35). Source: https://pubchem.ncbi.nlm.nih.gov.

2.1. Ligand-protein complex.

The coupling of amide analogs (1-23) with the IRAK-4 surface was determined using 5uit protein (https://doi.org/10.2210/pdb5UIT/pdb) [20] as a theoretical tool. Besides, PF-3758309, 336113-53-2, 509093-47-4, ND-2158, and emavusertib drugs were used as controls in DockingServer software (https://www.dockingserver.com/web). This program uses the MMFF94 force field [21] for energy minimization of the ligand molecules (amine and furanonone derivatives). Gasteiger partial charges were added to the atoms involved in the ligand. In addition, the hydrogen atoms were fused, and the rotational bonds were defined.

On the other hand, affinity maps (grids) of 20×20×20 Å with a spacing of 0.375 Å were generated using the Autogrid program [22]. Furthermore, the AutoDock parameter set and distance-dependent dielectric functions were used to calculate the van der Waals and electrostatic terms. It is worth noting that the docking simulations were performed using the Lamarckian genetic algorithm (LGA) and the local search method of Solis & Wets [23]. The initial position, orientation, and torsions of the ligand molecules were randomly established. It is important to mention that each docking experiment was determined after a maximum of 250,000 energy evaluations, with 150 repetitions. Finally, a translation step size of 0.2 Å and quaternion and torsion step sizes of 5 were used during the study.

2.2. Pharmacokinetic analysis.

Pharmacokinetic data for amine (3, 9, 25, 33, and 36) and furanone analogs (1, 3, 7, 13, 27, 32, and 34) were determined using the SwissADME software. The SwissADME program is a theoretical tool used to evaluate the pharmacokinetics, pharmacological similarity, and chemical compatibility of small molecules [24, 25].

2.3. Toxicology degree.

Toxicology evaluation for amine (3, 9, 25, 33, and 36) and furanone derivatives (1, 3, 7, 13, 27, 32, and 34) was determined using the Gussar software [26]. The GUSAR software was developed to create models based on the association of chemical structure and toxicological activity of various compounds. In silico prediction of LD50 values for rats with four types of administration (oral, intravenous, intraperitoneal, subcutaneous, inhalation) by GUSAR software. The training sets were created based on data from SYMYX MDL Toxicity Database. They include the information about ~10000 chemical structures with data on acute rat toxicity represented on the LD50 values (log10 (mmol/kg)).

3. Results and Discussion

3.1. Ligand-protein complex.

Table 3 shows the different types of amino acid residues involved in the interaction of amino derivatives (1-43) and the controls (1-439 PF-3758309, 336113-53-2, 509093-47-4, ND-2158, and emavusertib drugs) with the 5iut protein surface. Besides, Figure 3 shows the coupling of controls with the 5iut protein surface.

Table 3. Amino acid residues involved in the coupling of amino derivatives and the controls with the 5-uit protein surface.

Compound	Aminoacid residues
PF-3758309	Met_{344}; Arg_{347}; Ile_{348}; Gly_{362}
336113-53-2	Arg_{334}; Val_{343}; Met_{344}; Arg_{347}; Ile_{348}; Ile_{364}
509093-47-4	Ile_{308}; Arg_{334}; Ala_{335}; Val_{343}; Ile_{364}; Pro_{366}
ND-2158	Arg_{347}; Gly_{362}
Emavusertib	Met_{344}; Ile_{348}
1	Ile_{308}; Arg_{334}; Thr_{342}; Val_{343}; Ile_{364}; Thr_{365}; Pro_{366}
2	Glu_{225}; Gln_{228}; Gln_{229}; Gln_{232}; Arg_{310}; Arg_{334}; Val_{349}
3	Arg_{310}; Val_{349}; Met_{355}; Ala_{359}; Ile_{364}
4	Ile_{308}; Arg_{310}; Ile_{348}; Val_{349}; Met_{355}; Ala_{359}; Ile_{364}; Ser_{368}; Asp_{369}
5	Ile_{308}; Arg_{310}; Ile_{348}; Val_{349}; Met_{355}; Ala_{359}; Ile_{364}; Thr_{365}; Ser_{368}; Asp_{369}
6	Ile_{308}; Arg_{310}; Ile_{348}; Val_{349}; Met_{355}; Ala_{359}; Glu_{363}; Ile_{364}; Ser_{368}; Asp_{369}
7	Glu_{225}; Gln_{228}; Gln_{229}; Gln_{232}; Gly_{331}; Leu_{332}; Arg_{347}; Val_{349}
8	Arg_{310}; Arg_{334}; Met_{344}; Arg_{347}; Ile_{348}; Met_{355}; Ala_{359}; Gly_{362}; Ile_{364}
9	Glu_{225}; Gln_{228}; Gln_{229}; Gln_{232}; Leu_{332}; Arg_{347}; Val_{349}

Compound	Aminoacid residues
10	Arg_{310}; Val_{349}; Met_{355}; Ala_{359}; Ser_{368}; Ser_{372}
11	Glu_{225}; Gln_{229}; Gln_{232}; Arg_{310}; Leu_{332}; Arg_{334}; Arg_{347}; Val_{349}
12	Glu_{225}; Gln_{228}; Gln_{229}; Gln_{232}; Arg_{310}; Gly_{331}; Leu_{332}; Arg_{334}; Val_{349}
13	Ile_{308}; Arg_{310}; Ala_{359}; Thr_{365}; Ser_{368}
14	Phe_{197}; Glu_{225}; Gln_{229}; Arg_{347}; Ile_{348}; Val_{349}
15	Arg_{310}; Ile_{348}; Glu_{363}; Ile_{364}; Ser_{368}
16	Glu_{225}; Gln_{228}; Gln_{229}; Gln_{232}; Arg_{310}; Leu_{332}; Arg_{334}
17	Arg_{310}; Ile_{348}; Val_{349}; Met_{355}; Ala_{359}; Ile_{364}
18	Glu_{225}; Gln_{228}; Gln_{229}; Gln_{232}; Arg_{334}; Arg_{347}
19	Arg_{310}; Ile_{348}; Ala_{359}; Glu_{363}; Ile_{364}; Ser_{368}
20	Arg_{310}; Ile_{348}; Ala_{359}; Glu_{363}; Ile_{364}
21	Arg_{310}; Ile_{348}; Val_{349}; Met_{355} Ala_{359}; Ile_{364}
22	Arg_{310}; Ile_{348}; Val_{349}; Ala_{359}; Gly_{362}; Ile_{364}; Ser_{368}; Asp_{369}; Ser_{372}
23	Ile_{308}; Arg_{310}; Val_{349}; Met_{355}; Ala_{359}; Ile_{364}; Ser_{368}; Asp_{369}
24	Gln_{228}; Gln_{229}; Arg_{310}; Leu_{332}; Arg_{334}; Arg_{347}; Val_{349}
25	Ile_{308}; Arg_{334}; Ala_{335}; Val_{343}; Ile_{364}; Pro_{366}
26	Arg_{310}; Arg_{334}; Arg_{347}; Val_{349}; Met_{355}; Ala_{359}; Glu_{363}; Ile_{364}
27	Arg_{310}; Arg_{334}; Met_{344}; Arg_{347}; Ile_{348}; Ile_{36}
28	Met_{344}; Ile_{364}
29	Arg_{310}; Ile_{348}; Val_{349}; Met_{355}; Ala_{359}; Ile_{364}; Ser_{368}
30	Ile_{308}; Arg_{310}; Ala_{359}; Ser_{368}; Asp_{369}; Ser_{372}
31	Ile_{308}; Arg_{310}; Ile_{348}; Ala_{359}; Ile_{364}; Ser_{368}; Asp_{369}; Ser_{372}
32	Ile_{308}; Arg_{310}; Ile_{348}; Met_{355}; Ala_{359}; Ile_{364}; Ser_{368}; Asp_{369}
33	Arg_{310}; Ala_{359}; Ser_{368}; Asp_{369}; Ser_{372}
34	Arg_{310}; Arg_{334}; Arg_{347}; Ile_{348}; Ala_{359}; Ile_{364}
35	Phe_{197}; Glu_{225}; Gln_{229}; Gln_{232}; Arg_{310}; Leu_{332}; Arg_{332}; Arg_{347}; Val_{349}
36	Ile_{308}; Arg_{310}; Met_{355}; Ala_{359}; Ile_{364}; Thr_{365}; Ser_{368}; Asp_{369}; Ser_{372}
37	Ile_{308}; Arg_{310}; Ala_{359}; Ile_{364}; Thr_{365}; Ser_{368}; Asp_{369}
38	Arg_{310}; Met_{344}; Ile_{348}; Val_{349}; Met_{355}; Ala_{359}; Glu_{363}; Ile_{364}; Ser_{368}
39	Arg_{310}; Ile_{348}; Val_{349}; Met_{355}; Ala_{359}; Ile_{364}; Ser_{368}; Ser_{372}
40	Arg_{310}; Arg_{334}; Ile_{348}; Val_{349}; Ala_{359}; Gly_{362}; Ile_{364}
41	Ile_{308}; Arg_{334}; Ala_{359}; Ser_{336}; Val_{343}; Ile_{364}
42	Arg_{310}; Ile_{348}; Val_{349}; Met_{355}; Ala_{359}; Glu_{363}; Ile_{364}; Ser_{368}
43	Arg_{310}; Met_{344}; Ile_{348}; Val_{349}; Met_{355}; Ala_{359}; Ile_{364}

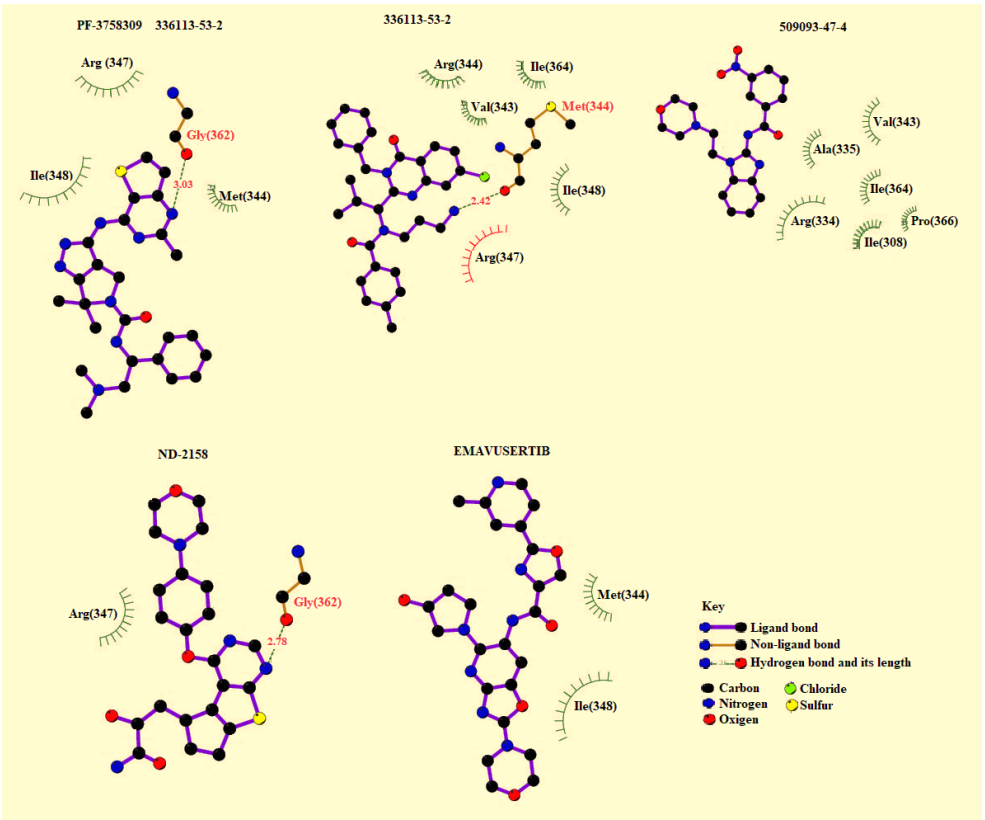

Figure 3. Couplig of PF-3758309, 336113-53-2, 509093-47-4, ND-2158, and emavusertib drugs with 5uit protein surface. Visualized with the DockingServer program.

3.2. Thermodynamic parameters.

Table 4 displayed the energy levels and inhibition constant (Ki) involved in the coupling of amino analogs (1-43), PF-3758309, 336113-53-2, 509093-47-4, ND-2158, and emavusertib (controls) with the 5uit protein surface. Besides, Figure 4 shows the energy levels for the amino derivative (3, 9, 25, 33, and 36) and the controls involved in the ligand-protein complexes formation. Finally, it is important to note that the inhibition constants for compounds 1, 9, 25, 33, and 36 were lower than those of the controls.

Table 4. Thermodynamic parameters involved in the coupling of amino derivatives (1-43), and the controls (PF-3758309, 336113-53-2, 509093-47-4, ND-2158, and emavusertib) with the 5uit protein surface.

Compound	A	B	C	D	E	F
PF-3758309	-4.22	809.09	-4.88	-0.36	-5.25	628.24
336113-53-2	-1.44	88.24	-5.79	0.22	-5.57	743.36
509093-47-4	-5.14	170.06	-5.90	-0.01	-5.91	578.91
ND-2158	-3.83	1.57	-4.22	0.00	-4.22	663.10
Emavusertib	-4.01	1.15	-4.39	0.14	-4.25	518.51
1	-3.64	2.89	-4.95	0.25	-4.70	589.33
2	-4.65	548.65	-3.13	-0.77	-3.90	485.63
3	-4.06	1.06	-4.52	-0.43	-4.95	345.57
4	-5.56	83.46	-5.77	-0.09	-5.86	421.65
5	-4.43	570.56	-4.64	-0.09	-4.72	409.57
6	-5.47	98.61	-5.68	-0.09	-5.76	407.77
7	-4.22	813.01	-5.15	0.04	-5.11	595.15
8	-4.98	224.96	-6.08	-0.04	-6.13	681.64
9	-4.06	1.05	-4.88	-0.08	-4.97	611.84
10	-4.19	844.23	-4.66	-0.43	-5.09	348.87
11	-4.65	388.24	-5.68	-0.05	-5.73	619.70
12	-3.55	2.48	-4.50	0.24	-4.27	585.48
13	-3.44	3.01	-3.65	-0.09	-3.74	301.11
14	-1.13	147.97	-3.05	-1.29	-4.34	400.88
15	-5.56	84.69	-6.28	-0.13	-6.41	426.32
16	-4.48	519.61	-4.83	-0.52	-5.35	509.29
17	-3.56	2.48	-4.25	-0.24	-4.49	334.79
18	-1.32	107.80	-4.82	0.45	-4.37	698.95
19	-3.61	2.27	-4.51	0.23	-4.27	412.09
20	-3.56	2.47	-4.06	-0.09	-4.15	344.05
21	-4.51	493.43	-5.03	-0.08	-5.10	579.98
22	-5.31	127.46	-5.94	0.02	-5.91	540.76
23	-5.71	65.76	-5.93	-0.08	-6.00	317.87
24	-5.13	173.51	-6.33	-0.01	-6.34	657.42
25	-4.03	1.11	-5.26	-0.08	-5.34	499.69
26	-5.93	45.02	-6.67	-0.16	-6.82	559.63
27	-4.35	648.21	-4.93	-0.31	-5.24	598.68
28	-4.13	942.25	-4.08	0.14	-3.94	560.01
29	-4.31	696.19	-4.55	-0.06	-4.61	389.58
30	-3.40	3.19	-3.72	-1.04	-4.31	297.28
31	-4.75	327.43	-6.14	-0.03	-6.18	499.92
32	-4.23	789.49	-4.49	-0.91	-5.40	404.46
33	-4.07	1.05	-4.29	-0.94	-5.23	351.65
34	-4.39	607.65	-4.94	-0.06	-5.00	573.35
35	-4.55	462.20	-5.45	0.00	-5,45	600.65
36	-3.86	1.48	-4.80	0.03	-4.77	425.92
37	-4.62	413.34	-4.73	-0.18	-4.91	349.63
38	-6.52	16.60	-7.69	0.08	-7.61	620.71
39	-4.82	293.99	-5.64	-0.36	-5.70	428.50
40	-4.34	663.58	-4.99	0.07	-4.92	546.37
41	-4.77	317.45	-5.52	-0.18	-5.70	461.80
42	-6.02	38.99	-6.51	-0.13	-6.64	431.38
43	-5.04	203.27	-5.95	0.01	-5.93	530.17

A = Est: free energy of binding (kcal/mol); B = Inhibition constant (Ki, mM); C = vdW + Hbond + desolv energy (kcal/mol); D = Electrostatic energy (kcal/mol); E = Total intermolec. energy (kcal/mol); F= Interact. surface.

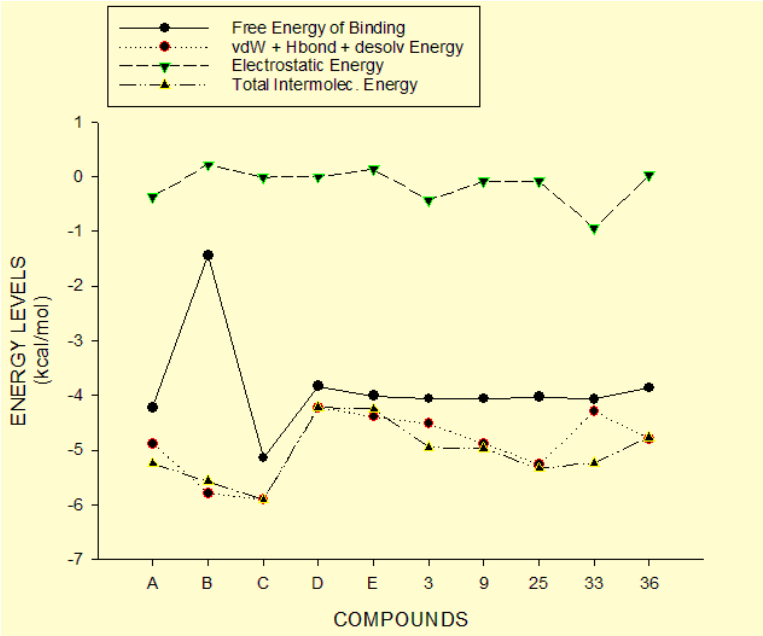

Figure 4. Energy levels for amino derivatives (3, 9, 25, 33, and 36) and controls (A-E).A = PF-3758309; B = 336113-53-2; C = 509093-47-4; D =ND-2158; E = Emavusertib.

3.3. Bond type.

Figure 5 and Table 5 show differences in the types of bonds involved in the coupling of amino derivatives (3, 9, 25, 33, and 36) with the 5-uit protein surface. Besides, Table 6 shows the decomposed interaction energies involved in the formation of the amino-5-uit protein complex for amino derivatives 3, 9, 25, 33, and 36.

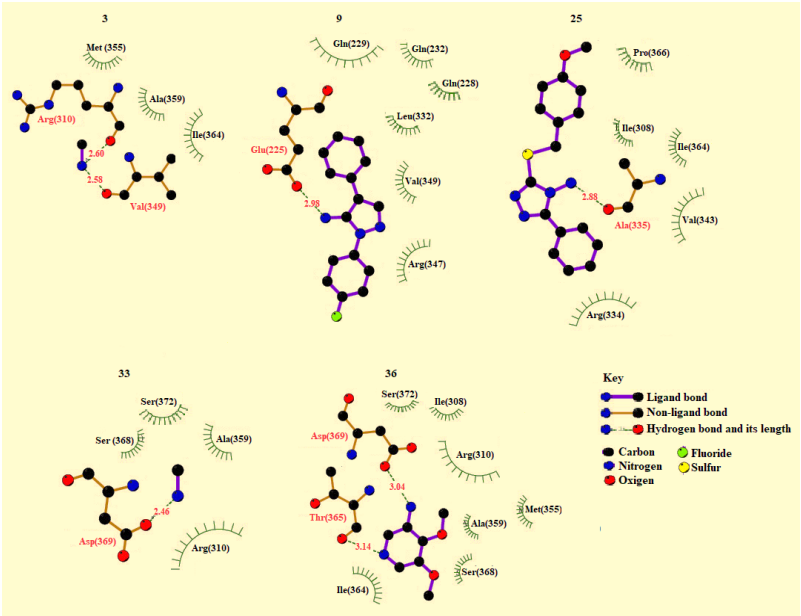

Figure 5. Coupling of amino derivatives (3, 9, 25, 33, and 36) with the 5uit protein surface. Visualized with DockingServer.

Table 5. Bond type and distance levels involved in the interaction of amino derivatives with the 5uit protein surface.

Compound	Hydrogen bond	Polar bond	Hydrophobic bond
3	Arg_{310} (N_1, 2.60) Val_{349} (N_1, 2.58)	Arg_{310} (H_{20}, 2.77)	Ala_{359} (C_6, 3.24) Ile_{364} (C_6, 3.76)
9	Glu_{225} (N_3, 2.62) Glu_{225} (H_2, 2.98) Glu_{225} (H_3, 3.05)	Gln_{229} (N_1, 3.44) Gln_{229} (N_1, 3.45)	Leu_{332} (C_1, 3.19) Val_{349} (C_{10}, 3.49)

Compound	Hydrogen bond	Polar bond	Hydrophobic bond
	Gln_{228} (H_3, 3.77)		
25	Ala_{335} (N_4, 2.88)	Arg_{334} (O_1, 3.42)	Ile_{308} (C_6, 3.16) Ile_{308} (C_7, 3.22) Val_{343} (C_{14}, 3.34) Val_{343} (C_{16}, 3.46) Val_{343} (C_8, 3.49) Ile_{364} (C_{16}, 3.34) Ile_{364} (C_7, 3.57) Pro_{366} (C_6, 3.79)
33	Asp_{369} (N_1, 2.46)	Asp (H_{23}, 2.12) Ser_{372} (H_{23}, 3.60) Arg_{310} (H_{23}, 3.66)	Ala_{359} (C_7, 3.41)
36	Asp_{369} (N_2, 3.04) Thr_{365} (N_1, 3.14) Asp_{369} (H_4, 3.61) Asp_{369} (H_3, 3.82) Ser_{368} (H_4, 3.24) Ser_{368} (H_3, 3.65)	Ser_{368} (N_1, 3.73) Arg_{310} (O_2, 3.84)	Ile_{308} (C_1, 3.29) Ile_{364} (C_6, 3.74) Ala_{359} (C_7, 3.18) Ala_{359} (C_4, 345) Ala_{359} (C_3, 3.57) Met_{355} (C_7, 3.44)

Table 6. Decomposed Interaction Energies in kcal/mol involved in the amino-5-uit protein complex formation.

Compound	Hydrogen bond	Polar Bond	Hydrophobic bond	Other
3	Arg_{310} (-0.892) Val_{349} (-0.0487)	Ile_{364} (-0.5496) Ala_{359} (-0.298)		Met_{355} (-0.2804)
9	Glu_{225} (-0.9881)	Gln_{229} (-1.6033)	Val_{349} (-0.5322) Leu_{332} (-0.2849)	Gln_{232} (-0.4896) Gln_{228} (-0.252)
25	Ala_{335} (-0.3097)	Arg_{334} (-0.8028)	Val_{343} (-0.6088) Ile_{364} (-0.2334) Pro_{366} (-0.2163) Ile_{308} (-0.0661)	
33	Asp_{369} (-0.2255)	Arg_{310} (-0.7019) Ser_{372} (-0.1278)	Ala_{359} (-0.1938)	Ser_{368} (-0.109)
36	Asp_{369} (-0.6573) Thr_{365} (-0.4893)	Arg_{310} (-1.2485) Ser_{368} (-0.2375) Ser_{372} (-0.1706)	Ile_{3764} (-0.5409) Ile_{308} (-0.2647) Met_{355} (-0.2527) Ala_{359} (-0.1317)	

3.4. Furanone analogs coupling.

Table 7 shows the differences in amino acid residues involved in the interaction of furanone analogs, 1-439 PF-3758309, 336113-53-2, 509093-47-4, ND-2158, and emavusertib (controls) with the 5iut protein surface.

Table 7. Amino acid residues involved in the coupling of furanone derivatives (1-35), and the controls (PF-3758309, 336113-53-2, 509093-47-4, ND-2158, and emavusertib) with the 5uit protein surface.

Compound	Aminoacid residues
PF-3758309	Met_{344}; Arg_{347}; Ile_{348}; Gly_{362}
336113-53-2	Arg_{334}; Val_{343}; Met_{344}; Arg_{347}; Ile_{348}; Ile_{364}
509093-47-4	Ile_{308}; Arg_{334}; Ala_{335}; Val_{343}; Ile_{364}; Pro_{366}
ND-2158	Arg_{347}; Gly_{362}
Emavusertib	Met_{344}; Ile_{348}
1	Phe_{197}; Glu_{225}; Gln_{228}; Gln_{229}; Gln_{232}; Leu_{332}; Arg_{334}; Arg_{347}; Val_{349}
2	Glu_{225}; Gln_{228}; Gln_{229}; Arg_{310}; Leu_{332}; Arg_{347}; Val_{349}
3	Arg_{310}; Met_{355}; Ala_{359}; Ser_{368}
4	Ile_{308}; Arg_{310}; Ile_{348}; Val_{349}; Met_{355}; Ala_{359}; Glu_{363}; Thr_{365}; Ser_{368}
5	Ile_{308}; Arg_{334}; Val_{343}; Ile_{364}
6	Arg_{310}; Arg_{334}; Ile_{348}; Ile_{364}
7	Arg_{310}; Arg_{334}; Ile_{348}; Ile_{364}
8	Phe_{197}; Glu_{225}; $_{225}$; Gln_{228}; Gln_{229}; Gln_{232}; $Arg_{310;}$ Leu_{332}; Arg_{347}; Val_{349}
9	Glu_{225}; Gln_{228}; Gln_{229}; Gln_{232}; Arg_{310}; Arg_{334}; Arg_{347}; Val_{349}
10	Ile_{308}; $Arg_{310;}$ Ala_{359}; Ser_{368}
11	$Arg_{310;}$ Met_{355}; Ala_{359}; Ser_{368}; Asp_{369}; Ser_{372}
12	Ile_{308}; Arg_{334}; Ala_{335}; Val_{343}; Ile_{364}
13	Ile_{308}; Arg_{310}; Val_{349}; Met_{355}; Ala_{359}; Ile_{364}; Thr_{365}; Ser_{368}; Asp_{369}
14	Ile_{308}; Arg_{310}; Val_{349}; Ala_{359}; Glu_{363}; Ile_{364}; Ser_{368}; Asp_{369}
15	Ile_{308}; $Arg_{334;}$ Ala_{335}; Val_{343}; Ile_{364}

Compound	Aminoacid residues
16	Ile308; Arg334; Ala335; Val343; Ile364
17	Arg334; Val343; Ile348; Ile364
18	Arg310; Ala359; Ile364; Ser368
19	Phe197; Gln228; Gln229; Arg310; Leu332; Arg334; Arg347; Val349
20	Ile308; Arg310; Ala359; Ser368
21	Arg310; Arg347; Ile348; Gly362; Ile364
22	Il308; Val343; Ile364
23	Arg310; Ile348; Met355; Ala359; Ile364; Ser368; Asp369; Ser372
24	Arg310; Met344; Ile348; Gly362; Ile364
25	Arg310; Arg334; Ile364
26	Arg310; Arg334; Met344; Ile348; Ile364
27	Arg310; Arg334; Ile364
28	Ile308; Arg310; Ile348; Ala359; Ile364; Ser368
29	Arg334; Val343; Met344; Arg347; Ile364
30	Arg310; Ala359; Glu363; Ser368
31	Arg310; Arg334; Ile348; Ile364
32	Arg310; Met355; Ala359; Thr365; Ser368; Asp369
33	Gln229; Gln232; Arg310; Leu332; Arg334; Val349
34	Ile308; Arg310; Met355; Ala359; Ser368; Asp369; Ser372
35	Arg310; Ile348; Met355; Ala359; Ile364

3.5. Energy levels.

Table 8 displays the energy levels and inhibition constants (Ki) for the coupling of furanone analogs (1-43), PF-3758309, 336113-53-2, 509093-47-4, ND-2158, and emavusertib (controls) with the 5uit protein surface. Besides, Figure 6 shows the energy levels for furanone derivative (1, 3, 7, 13, 24, 27, 32, and 34) and the controls involved in the ligand-protein complexes formation. It is noteworthy that the inhibition constants for compounds 1, 3, 9, 25, 33, and 36 were lower than those of the controls.

Table 8. Thermodynamic parameters involved in the coupling of furanone derivatives (1-34), (PF-3758309, 336113-53-2, 509093-47-4, ND-2158, and emavusertib) with the 5uit protein surface.

Compound	A	B	C	D	E	F
PF-3758309	-4.22	809.09	-4.88	-0.36	-5.25	628.24
336113-53-2	-1.44	88.24	-5.79	0.22	-5.57	743.36
509093-47-4	-5.14	170.06	-5.90	-0.01	-5.91	578.91
ND-2158	-3.83	1.57	-4.22	0.00	-4.22	663.10
Emavusertib	-4.01	1.15	-4.39	0.14	-4.25	518.51
1	-3.95	1.27	-5.48	-0.15	-5.53	679.05
2	-3.13	5.09	-4.77	-0.32	-5.09	593.06
3	-3.87	1.47	-3.61	-0.04	-3.65	326.96
4	-4.92	248.83	-4.84	-0.08	-4.92	309.30
5	-4.25	772.46	-4.57	0.02	-4.54	462.02
6	-4.33	73.13	-3.03	-1.30	-4.33	415.86
7	-3.91	1.37	-2.87	-1.34	-4.21	482.72
8	-4.38	616.43	-5.14	-0.12	-5.26	731.59
9	-4.65	393.66	-5.47	-0.13	-5.60	654.34
10	-3.63	2.18	-3.63	0.00	-3.63	311.99
11	-4.38	612.20	-4.53	0.14	-4.38	344.76
12	-4.38	618.40	-5.36	0.06	-5.30	567.28
13	-3.98	1.21	-4.64	0.03	-3.98	284.23
14	-4.99	22.91	-5.09	0.11	-4.99	361.59
15	-4.12	947.43	-4.74	-0.04	-4.77	455.85
16	-4.89	259.26	-5.33	-0.08	-5.41	447.03
17	-3.28	3.98	-4.52	0.08	-4.44	642.11
18	-4.26	759.27	-4.81	-0.03	-4.84	370.93
19	-4.29	719.32	-4.83	-0.07	-4.90	623.38
20	-3.45	2.97	-3.34	-0.11	-3.45	308.73
21	-4.47	533.36	-4.90	0.14	-4.75	518.22
22	-3.51	2.68	-3.18	-0.86	-4.05	390.66
23	-5.05	199.52	-5.74	-0.08	-5.80	454.15
24	-4.07	1.05	-4.22	-0.30	-4.52	542.57
25	-4.16	898.44	-2.58	-1.60	-4.16	418.86

Compound	A	B	C	D	E	F
26	-4.66	384.32	-3.85	-1.42	-5.27	530.52
27	-3.64	1.29	-2.41	-1.53	-3.94	368.54
28	-3.37	3.41	-3.57	-0.09	-3.66	335.99
29	-4.63	402.89	-4.57	-0.08	-4.65	616.11
30	-4.71	351.17	-5.11	0.09	-5.01	360.62
31	-4.27	743.06	-3.45	-1.12	-4.57	466.70
32	-3.69	1.19	-4.17	-0.12	-4.29	392.92
33	-3.60	2.28	-3.49	-0.11	-3.80	457.26
34	-3.95	1.28	-3.11	-1.14	-4.25	299.48
35	-3.18	-4.65	-2.99	-0.20	-3.18	295.46

A = Est: free energy of binding (kcal/mol); B = Inhibition constant (Ki, mM); C = vdW + Hbond + desolv energy (kcal/mol); D = Electrostatic energy (kcal/mol); E = Total intermolec. energy (kcal/mol); F= Interact. Surface.

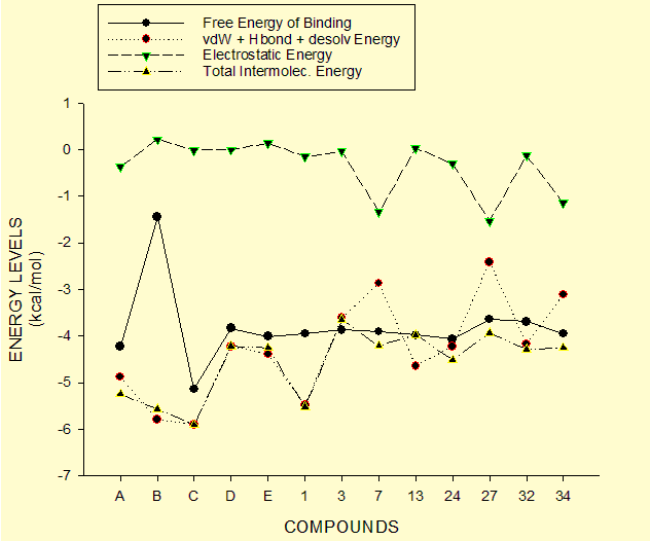

Figure 6. Energy levels for furanone derivatives (1, 3, 7, 13, 24, 27, 32, and 34) and controls (A-E). A = PF-3758309; B = 336113-53-2; C = 509093-47-4; D =ND-2158; E = Emavusertib.

3.6. Bond type.

Table 9 and Figure 7 show differences in the types of bonds involved in the coupling of furanone analogs (1, 3, 7, 13, 24, 27, 32, and 34) with the 5uit protein surface.

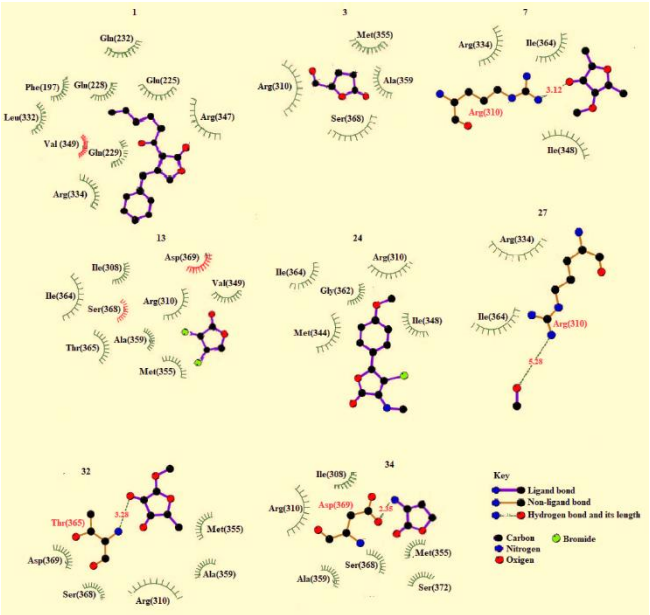

Figure 7. Interaction of furanone analogs (1, 3, 7, 13, 24, 27, 32, and 4) with the 5uit protein surface. Visualized with DockingServer.

Table 9. Bond type and distance levels involved in the coupling of furanone derivatives with the 5uit protein surface.

Compound	Hydrogen bond	Polar bond	Hydrophobic bond	Halogen bond
1		Gln_{229} (O_3, 3.62)	Leu_{332} (C_{13}, 3.58) Val_{349} (C_{13}, 3.22) Val_{349} (C_{12}, 3.26) Val_{349} (C_{11}, 3.32)	
3		Arg_{310} (O_8, 3.41) Arg_{310} (H_{14}, 3.85)	Ala_{359} (C_7, 3.59)	
7	Arg_{310} (O_3, 3.10)	Arg_{334} (O_3, 3.56)	Ile_{364} (C_6, 3.45) Ile_{364} (C_4, 3.89)	
13		Arg_{310} (O_8, 3.38)	Ala_{359} (C_5, 3.38)	Asp_{369} (Br, 3.11) Arg_{310} (Br, 3.14) Val_{349} (Br, 3.39) Thr_{365} (Br, 3.88)
24		Arg_{310} (O_3, 3.09)	Ile_{348} (C_{10}, 3.06) Ile_{348} (C_{11}, 3.40) Ile_{364} (C_8, 3.36) Ile_{364} (C_9, 3.90) Ile_{364} (C_{12}, 3.69)	Gly_{362} (Br, 3.56)
27	Arg_{310} (O, 3.18)	Arg_{334} (O, 3.34)	Ile_{364} (C, 3.58)	
32	Thr_{365} (O_3, 3.28)	Arg_{310} (O_3, 3.74) Arg_{310} (O_4, 3.89) Asp_{369} (O_2, 3.26)	Ala_{359} (C_6, 3.40) Ala_{359} (C_2, 3.48) Ala_{359} (C_3, 3.83) Met_{355} (C_6, 3.73)	Arg_{310} (C_3, 3.64) Arg_{310} (C_4, 3.63) Arg_{310} (C_1, 3.56) Arg_{310} (C_2, 3.67) Arg_{310} (C_5, 3.64) Ala_{359} (O_1, 3.39) Ala_{359} (O_4, 3.85) Ser_{368} (C_4, 3.53) Ser_{368} (O_2, 3.11)
34	Asp_{369} (N_6, 2.35) $Ile_{3.08}$ (H_{15}, 3.58) Arg_{310} (H_{15}, 3.77) Ser_{368} (H_{15}, 3.66) Asp_{369} (H_{15}, 3.20)	Arg_{310} (O, 3.39)	Met_{355} (C_5, 3.21) Ala_{359} (C_5, 3.73)	

Finally, Table 10 shows the decomposed Interaction Energies for furanone derivatives (1, 3, 7, 13, 24, 27, 32, and 34).

Table 10. Decomposed Interaction Energies in kcal/mol involved in the ligand-protein complex formation.

Compound	Hydrogen bond	Polar Bond	Hydrophobic bond	Other
1		Gln_{229} (-0.4762)		Arg_{347} (-1.3044) Glu_{225} (-0.8725) Arg_{334} (-0.7681) Gln_{232} (-0.626) Gln_{228} (-0.4601)
3		Arg_{310} (-1.05)	Ala_{359} (-0.4453)	Met_{355} (-0.2877) Ser_{368} (-0.1567)
7		Arg_{310} (-0.4269) Arg_{334} (-0.3643)	Ile_{364} (-0.2735)	Ile_{348} (-0.6681)
13	Arg_{310} (-0.4295) Thr_{365} (-0.3427) Val_{349} (-0.2212) A_{310} (-0.4269)			
24	Gly_{362} (-0.0762)	Arg_{310} (-0.6309)	Ile_{364} (-0.4625) Ile_{348} (-0.3579)	Met_{344} (-0.5945)
27	Arg_{310} (-0.4053)	Arg_{334} (-0.5675)	Ile_{364} (-0.4622)	
32	Thr_{365} (-0.471)	Arg_{310} (-0.9801) Asp_{369} (-0.2814)	Met_{355} (-0.3027) Ala_{359} (-0.2367)	Ser_{368} (-0.2003)
34	Asp_{369} (-0.8202)	Arg_{310} (-0.7167)	Met_{355} (-0.1202) Ala_{359} (-0.1796)	Ser_{372} (-0.1917) Ile_{308} (-0.1457) Ser_{368} (-0.0758)

3.7. Pharmacokinetic parameters.

The pharmacokinetic values for amino derivatives 3, 9, 25, 33, and 36 are shown in Table 11 using the SwissADME program. The results showed that compounds 3, 33, and 36 lack affinity for all CYPs studied (Table 9).

Table 11. Pharmacokinetic parameters for amino derivatives (3, 9, 25, 33, and 36).

Compound	*A*	*B*	*C*	*D*	*E*	*F*	*G*	*H*	*I*
3	High	Yes	No	No	No	No	No	No	1.06
9	High	Yes	No	Yes	Yes	No	No	No	3.11
25	High	No	No	Yes	Yes	Yes	No	No	2.82
33	High	Yes	No	No	No	No	No	No	1.45
36	High	Yes	No	No	No	No	No	No	0.45

A = GI absorption; *B* = BBB permeant; *C* = P-GP substrate; *D* = CYP1A2 inhibitor; *E* = CYP2C19 inhibitor; *F* = YP2C9 inhibitor; *G* = CYP2D6 inhibitor; *H*= CYP3A4 inhibitor; *I* = Consensus $LogP_{O/W}$

Other results showed that furanone analogs 3, 27, 32, and 34 lack affinity for all CYPs studied (Table 12).

Table 12. Pharmacokinetic factors for furanone analogs (1, 3, 7, 13, 24, 27, 32, and 34).

Compound	*A*	*B*	*C*	*D*	*E*	*F*	*G*	*H*	*I*
1	High	Yes	No	Yes	Yes	Yes	No	No	3.15
3	High	No	No	No	No	No	No	No	-0.07
7	High	Yes	No	No	No	No	No	No	0.92
13	High	Yes	No	No	No	No	No	No	1.61
24	High	Yes	No	Yes	Yes	No	No	No	2.09
27	High	No	No	No	No	No	No	No	0.27
32	High	No	No	No	No	No	No	No	0.25
34	High	No	No	No	No	No	No	No	-0.22

A = GI absorption; *B* = BBB permeant; *C* = P-GP substrate; *D* = CYP1A2 inhibitor; *E* = CYP2C19 inhibitor; *F* = CYP2C9 inhibitor; *G* = CYP2D6 inhibitor; *H*= CYP3A4 inhibitor; *I* = Consensus Log $P_{O/W}$.

Finally, Tables 13 and 14 showed the theoretical toxicity degree for amino and furanone derivatives.

Table 13. Toxicity degree analysis produced by amino derivatives (3, 9, 25, 33, and 36) using the Gussar program.

Compuesto	IP LD_{50} (mg/kg)	IV LD_{50} (mg/kg)	Oral LD_{50} (mg/kg)	SC LD_{50} (mg/kg)
3	260.80	70.28	588.60	389.80
9	571.70	196.40	638.40	567.00
25	493.20	123.60	1357.00	974.40
33	121.60	71.83	1024.00	426.60
36	245.10	141.60	552.70	337.90

IP - Intraperitoneal route of administration; IV - Intravenous route of administration; Oral - Oral route of administration; SC - Subcutaneous route of administration.

Table 14. Toxicity degree analysis produced by furanone analogs (1, 3, 7, 13, 24, 27, 32, and 34) using the Gussar program.

Compuesto	IP LD_{50} (mg/kg)	IV LD_{50} (mg/kg)	Oral LD_{50} (mg/kg)	SC LD_{50} (mg/kg)
1	122.00	28.43	1459.00	377.40
3	490.60	375.70	2994.00	1263.00
7	263.20	40.96	872.00	651.50
13	903.10	47.30	1179.00	1641.00
24	857.30	70.62	1723.00	2142.00
27	186.00	46.95	1094.00	280.60
32	181.40	67.78	1322.00	522.80
34	172.30	41.45	1268.00	457.10

IP - Intraperitoneal route of administration; IV - Intravenous route of administration; Oral - Oral route of administration; SC - Subcutaneous route of administration.

3.8. Discussion.

IRAK-4 is a biomolecule involved in cell signaling, inflammation, apoptosis, and cell differentiation. Notably, IRAK-4 has been associated with various types of cancer and autoimmune diseases, leading to the development of several IRAK-4 inhibitors for the treatment of these clinical pathologies [27-31]. However, more selective inhibitors are needed for the treatment of chronic lymphocytic leukemia to reduce some of the side effects produced by IRAK-4 inhibitors. For this reason, this study aimed to determine the interaction of several compounds (with amino and furan functional groups) with IRAK-4 as a possible therapeutic alternative for the treatment of chronic lymphocytic leukemia, as follows:

3.8.1. Amino derivative-protein complex.

Several methods have been reported for determining the interactions of various drugs (ligands) with different biomolecules, including SwissDock [32], DockThor-VS [33], AutoDock [34], GlideWS [35], Gold [36], X-Dock [37], and DockingServer [38]. In this study, the possible interaction of some amino and furanone derivatives with IRAK-4 was determined using the 5uit protein as a theoretical tool. Besides, 1-439 PF-3758309, 336113-53-2, 509093-47-4, ND-2158, and emavusertib drugs were used as controls in the DockinServer program. The results showed differences in the amino acid residues involved in interactions between amine derivatives (compounds 1-43) and the 5uit protein surface compared to the controls. This phenomenon could lead to changes in the biological activity of IRAK-4, associated with different energy levels during the interaction of amine derivatives with IRAK-4. For this reason, the energy levels involved in the interaction of amine derivatives with the 5uit protein were determined using DockingServer. The results showed that free energy for binding was lower for amino derivatives 3, 9, 25, 33, and 36 compared with the 336113-53-2 drug. However, the free energy of binding for these amino derivatives was higher in comparison with the 509093-47-4 drug. Finally, the free energy of binding for compounds 3, 9, 25, 33, and 36 was in a manner similar to the PF-3758309, ND-2158, and Emavusertib drugs. Besides, the inhibition constants were lower for amino derivatives 3, 9, 25, 33, and 36 than for the PF-3758309, 336113-53-2, 509093-47-4, ND-2158, and emavusertib drugs. This phenomenon could be due to different types of bonds involved in the ligand-protein formation complex between amino derivatives and the 5uit protein. The results showed that amino derivatives 33 and 36 may interact with amino acid residues Asp369 via hydrogen bonds and with Arg310, compared with amino analogs 3, 9, and 25. These results indicate that compounds 3, 9, 25, 33, and 36 may alter the biological activity of IRAK-4, potentially decreasing the development of chronic lymphocytic leukemia, and this effect may depend on the chemical structure of each amino derivative. Analyzing this hypothesis, this study determined the coupling of furanone analogs with the 5UIT protein surface to characterize whether these compounds could have an affinity for IRAK-4 as follows:

3.8.2. Furanone derivative-protein complex.

The results show differences in the amino acid residues involved in the interactions of furanone analogs (compounds 1-34) with the 5uit protein surface compared with those of the PF-3758309, 336113-53-2, 509093-47-4, ND-2158, and emavusertib drugs. Other data

indicate that the inhibition constant was lower for the compounds 1, 3, 7, 13, 27, 32, and 34 compared with PF-3758309, 336113-53-2, 509093-47-4, ND-2158, and emavusertib. These data suggest that compounds 1, 3, 7, 13, 27, 32, and 34 may have higher affinity for the 5uit protein surface. This phenomenon could be conditioned by some thermodynamic parameters involved in the ligand-protein formation. For this reason, the energy levels were determined; the results showed that the free energy of binding for furanone derivatives 1, 3, 7, 13, 27, 32, and 34 was higher compared to the 509093-47-4 drug. Besides, the binding free energy of furanone derivatives was lower than that of the 336113-53-2 drug. Finally, the free energy of binding for compounds 3, 9, 25, 33, and 36 was in a manner similar to the PF-3758309, ND-2158, and Emavusertib drugs.

On the other hand, the different types of chemical bonds could condition the coupling of furanone derivatives with the surface of the 5uit protein. In this way, the amino acid residue Arg 310 appears to be important in the coupling of compounds 3, 24, 27, 32, and 34 to the 5uit protein surface via polar bonds, compared to furanone derivatives 7 and 13. All these suggest that furanone derivatives 1, 3, 7, 13, 27, 32, and 34 could produce changes in biological activity, and this phenomenon may inhibit the activity of IRAK-4; however, it is important to mention that it is necessary to determine their biological activity using an in vivo or in vitro model. For this reason, some pharmacokinetic parameters of the amino and furanone derivatives were analyzed, as follows:

3.8.3. Pharmacokinetic parameters.

Several methods have been used to determine some pharmacokinetic parameters associated with the biological activity of different drugs, such as GastroPlus@ [39], PKMP [40], NONMEM [41], PBPK [42], SwissADME [43], and others. In this study, SwissADME was used to predict the pharmacokinetic parameters of amine derivatives 3, 9, 25, 33, and 36. The results indicate that amine analogs may exhibit increased gastrointestinal absorption. Furthermore, the metabolism of amine derivatives 1 and 24 involves interaction with CYP1A2 and CYP2C19. However, compounds 3, 33, and 36 do not interact with the CYPs involved in this study. All these data suggest that CYP1A2 may significantly influence the metabolism of 1 and 24, affecting their efficacy and safety. This phenomenon is supported by data indicating that CYP1A2 plays an important role in the metabolism of several drugs [44]; for example, a study found that CYP1A2 accounts for 10-15% of the metabolism of drugs such as clozapine, olanzapine, and duloxetine [45]. Analyzing these data, in this study, some pharmacokinetic factors were determined for furanone analogs 3, 7, 13, 27, 32, and 34. The results showed that furanones 3, 7, 27, 32, and 34 may have higher gastrointestinal absorption. However, these compounds do not interact with the CYPs involved in this study; these data suggest that they could be metabolized by other biological systems, as is the case with aristolochic acid, which is metabolized by the human UDP-glucuronosyltransferase 1A enzyme to form a less nephrotoxic glucuronide [46].

3.8.4. Toxicology analysis.

For several years, several methods such as ToxCast [47], TOXII [48], GENETOX [49], Osiris [50], and Gussar [51] have been used to determine the degree of toxicity of different drugs. In this way, to evaluate the theoretical toxicity degree produced by some amine analogs (3, 9, 25, 33, and 36), the Gussar software was used. The results indicate that amine derivative

9 requires a higher dose to produce toxicity via the intraperitoneal route compared with the compounds 3, 25, 33, and 36. However, amino derivative 33 requires a higher dose to produce toxicity via the oral route. These data suggest that differences in the chemical structure of amino derivatives can produce changes in the degree of toxicity. This hypothesis is supported by toxicity studies on various amino-aromatic derivatives using the Jakel-Klein model [52].

On the other hand, a report showed that some furanone derivatives can produce different degrees of toxicity [53]; for this reason, in this study, the possible degree of toxicity produced by furanone derivatives (1, 3, 7, 13, 24, 27, 32, and 34) was calculated using the Gussar program. The results showed that furanone 3 may require a higher dose to produce toxicity via the oral route than 1, 7, 13, 24, 27, 32, and 34. Besides, the compound 24 requires a higher dose to produce toxicity via the intravenous route. These data indicate that the toxicity degree produced by furanones may depend on: 1) the dose and routes of administration, and 2) differences in the chemical structure of furanone derivatives.

4. Conclusions

In this study, we reported the interaction of some amine and furanone derivatives with IRAK-4 using the 5uit protein as a theoretical tool in the DockingServer program. The results indicated that amine (3, 9, 25, 33, and 36) and furanone (1, 3, 7, 13, 24, 27, 32, and 34) derivatives may have a higher affinity for the 5uit protein surface in comparison with the controls. These data indicate that both amine and furanone derivatives can act as IRAK-4 inhibitors, suggesting they are promising candidates for the treatment of chronic lymphocytic leukemia. However, further experiments using a biological model are needed to validate this hypothesis and rule out potential side effects of these compounds.

Author Contributions

Conceptualization, R.N.M. and A.-R.M.; data curation, R.N.M.; formal analysis, R.N.M., A.-R.M., M.-G.M.A. and R.-H.A.; funding acquisition, R.N.M., A.-R.M., B.-Z.E., M.-G.M.A. and R.-H.A.; investigation, R.N.M., A.-R.M., B.-Z.E., M.-G.M.A. and R.-H.A.; methodology, R.N.M., A.-R.M. and B.-Z.E.; visualization, R.N.M., A.-R.M., B.-Z.E., M.-G.M.A. and R.-H.A.; writing—original draft preparation, R.N.M. and A.-R.M.; writing—review and editing, R.N.M., A.-R.M., B.-Z.E., M.-G.M.A. and R.-H.A. All authors have read and agreed to the published version of the manuscript.

Institutional Review Board Statement

Not applicable.

Informed Consent Statement

Not applicable.

Data Availability Statement

The data that support the findings of this study are available from the corresponding author upon reasonable request.

Funding

The authors received no specific funding for this work.

Acknowledgments

None.

Conflicts of Interest

Authors declare no conflicts of interest.

References

1. Tinsley-Vance, S.; Reich, R.; Lastorino, D.; Durosier-Mertilus, D.; Zhang, Y. Predictors of health-related quality of life in adults with chronic lymphocytic leukemia or small lymphocytic lymphoma. *Blood* **2025**, *146*, 8108, https://doi.org/10.1182/blood-2025-8108.
2. Hallek, M. Chronic Lymphocytic Leukemia: 2025 Update on the Epidemiology, Pathogenesis, Diagnosis, and Therapy. *Am. J. Hematol.* **2025**, *100*, 450-480, https://doi.org/10.1002/ajh.27546.
3. Haddon, C.J. Quality of life in patients with monoclonal B-cell lymphocytosis or chronic lymphocytic leukaemia managed by active monitoring. *Cancer Nurs. Pract.* **2025**, *24*, https://doi.org/10.7748/cnp.2025.e1900.
4. Koehrer, S.; Burger, J.A. Chronic Lymphocytic Leukemia: Disease Biology. *Acta Haematol.* **2023**, *147*, 8-21, https://doi.org/10.1159/000533610.
5. Askari, F.; Khatami, M.; Heidari, M.M. Intracellular signaling pathways and molecular mechanisms contributed to the pathogenesis of acute and chronic types of Leukemia. *Cell. Mol. Biomed. Rep.* **2026**, *6*, 29-50, https://doi.org/10.55705/cmbr.2026.520569.1313.
6. Balla, B.; Tripon, F.; Lazar, E.; Bănescu, C. Analysis of Mutational Status of *IGHV*, and Cytokine Polymorphisms as Prognostic Factors in Chronic Lymphocytic Leukemia: The Romanian Experience. *Int. J. Mol. Sci.* **2024**, *25*, 1799, https://doi.org/10.3390/ijms25031799.
7. Fergany, A.; Hassanein, K.M.; Zahran, A.M.; Abdel Hameed, M.R.; Kamel, A.M. Clinical significance of interleukin 10, interleukin 33, and interleukin 35 on induction chemotherapy in acute myeloid leukemia patients. *Egypt. J. Haematol.* **2025**, *50*, 125-132, https://doi.org/10.4103/ejh.ejh_83_24.
8. Su, L.-C.; Xu, W.-D.; Huang, A.-F. IRAK family in inflammatory autoimmune diseases. *Autoimmun. Rev.* **2020**, *19*, 102461, https://doi.org/10.1016/j.autrev.2020.102461.
9. Bai, Y.-R.; Yang, W.-G.; Hou, X.-H.; Shen, D.-D.; Zhang, S.-N.; Li, Y.; Qiao, Y.-Y.; Wang, S.-Q.; Yuan, S.; Liu, H.-M. The recent advance of Interleukin-1 receptor associated kinase 4 inhibitors for the treatment of inflammation and related diseases. *Eur. J. Med. Chem.* **2023**, *258*, 115606, https://doi.org/10.1016/j.ejmech.2023.115606.
10. Vick, E.J.; Hassan, A.; Choi, K.; Bennett, J.; Muto, T.; Clough, C.A.; Culver-Cochran, A.E.; Hueneman, K.; Bolanos, L.C.; Wunderlich, M.; Zhang, X.; McKnight, C.; Ceribelli, M.; Holland, D.; Klumpp-Thomas, C.; Greis, K.D.; Thomas, C.J.; Starczynowski, D.T. Targeting of IRAK4 and GSPT1 enhances therapeutic efficacy in AML via c-Myc destabilization. *Leukemia* **2025**, *39*, 2163-2173, https://doi.org/10.1038/s41375-025-02695-3.
11. Smith, M.A.; Choudhary, G.S.; Pellagatti, A.; Choi, K.; Bolanos, L.C.; Bhagat, T.D.; Gordon-Mitchell, S.; Von Ahrens, D.; Pradhan, K.; Steeples, V.; Kim, S.; Steidl, U.; Walter, M.; Fraser, I.D.C.; Kulkarni, A.; Salomonis, N.; Komurov, K.; Boultwood, J.; Verma, A.; Starczynowski, D.T. U2AF1 mutations induce oncogenic IRAK4 isoforms and activate innate immune pathways in myeloid malignancies. *Nat. Cell Biol.* **2019**, *21*, 640-650, https://doi.org/10.1038/s41556-019-0314-5.
12. Parrondo, R.D.; Iqbal, M.; Von Roemeling, R.; Von Roemeling, C.; Tun, H.W. IRAK-4 inhibition: emavusertib for the treatment of lymphoid and myeloid malignancies. *Front. Immunol.* **2023**, 14, 1239082, https://doi.org/10.3389/fimmu.2023.1239082.
13. Li, Z.; Younger, K.; Gartenhaus, R.; Joseph, A.M.; Hu, F.; Baer, M.R.; Brown, P.; Davila, E. Inhibition of IRAK1/4 sensitizes T cell acute lymphoblastic leukemia to chemotherapies. *J. Clin. Investig.* **2015**, *125*, 1081-1097, https://doi.org/10.1172/JCI75821.

14. Wu, X.; Wang, L.; Qiu, Y.; Zhang, B.; Hu, Z.; Jin, R. Cooperation of IRAK1/4 inhibitor and ABT-737 in nanoparticles for synergistic therapy of T cell acute lymphoblastic leukemia. *Int. J. Nanomedicine* **2017**, *12*, 8025-8034, https://doi.org/10.2147/IJN.S146875.
15. Booher, R.; Samson, M.E.S.; Borek, M.; Modafferi, H.; Martell, R.E. PS991 CA-4948, An IRAK4/FLT3 Inhibitor, Shows Antileukemic Activity In Mouse Models of FLT3 wild-type and FLT3 Mutated Acute Myeloid Leukemia (AML). *HemaSphere* **2019**, *3*, 445-446, https://doi.org/10.1097/01.HS9.0000562260.56570.c7.
16. Garcia-Manero, G.; Platzbecker, U.; Tarantolo, S.R.; Gropper, S.; Talati, C.; Götze, K.S.; Dugan, J.; Winer, E.S.; Martinez, E.; Lieberman, C.; von Roemeling, R. A Phase 1, Open Label Dose Escalation Trial Evaluating the Safety, Pharmacokinetics, Pharmacodynamics, and Clinical Activity of Orally Administered CA-4948 in Patients with Acute Myelogenous Leukemia or Myelodysplastic Syndrome. *Blood* **2020**, *136*, 16, https://doi.org/10.1182/blood-2020-140889.
17. Bothe, U.; Günther, J.; Nubbemeyer, R.; Siebeneicher, H.; Ring, S.; Bömer, U.; Peters, M.; Rausch, A.; Denner, K.; Himmel, H.; Sutter, A.; Terebesi, I.; Lange, M.; Wengner, A.M.; Guimond, N.; Thaler, T.; Platzek, J.; Eberspächer, U.; Schäfer, M.; Steuber, H.; Zollner, T.M.; Steinmeyer, A.; Schmidt, N. Discovery of IRAK4 Inhibitors BAY1834845 (Zabedosertib) and BAY1830839. *J. Med. Chem.* **2024**, *67*, 1225-1242, https://doi.org/10.1021/acs.jmedchem.3c01714.
18. Isah, J.J.; Uzairu, A.; Uba, S.; Ibrahim, M.T. Novel design and in silico optimization of 5-azaquinazoline-based IRAK4 inhibitors using qsar, docking, pharmacokinetics, and molecular dynamics for diffuse large B-Cell lymphoma. *In Silico Res. Biomed.* **2025**, *1*, 100047, https://doi.org/10.1016/j.insi.2025.100047.
19. Von Roemeling, C.A.; Doonan, B.P.; Klippel, K.; Schultz, D.; Hoang-Minh, L.; Trivedi, V.; Li, C.; Russell, R.A.; Kanumuri, R.S.; Sharma, A.; Tun, H.W.; Mitchell, D.A. Oral IRAK-4 Inhibitor CA-4948 Is Blood-Brain Barrier Penetrant and Has Single-Agent Activity against CNS Lymphoma and Melanoma Brain Metastases. *Clin. Cancer Res.* **2023**, *29*, 1751-1762, https://doi.org/10.1158/1078-0432.CCR-22-1682.
20. Lee, K.L.; Ambler, C.M.; Anderson, D.R.; Boscoe, B.P.; Bree, A.G.; Brodfuehrer, J.I.; Chang, J.S.; Choi, C.; Chung, S.; Curran, K.J.; Day, J.E.; Dehnhardt, C.M.; Dower, K.; Drozda, S.E.; Frisbie, R.K.; Gavrin, L.K.; Goldberg, J.A.; Han, S.; Hegen, M.; Hepworth, D.; Hope, H.R.; Kamtekar, S.; Kilty, I.C.; Lee, A.; Lin, L.-L.; Lovering, F.E.; Lowe, M.D.; Mathias, J.P.; Morgan, H.M.; Murphy, E.A.; Papaioannou, N.; Patny, A.; Pierce, B.S.; Rao, V.R.; Saiah, E.; Samardjiev, I.J.; Samas, B.M.; Shen, M.W.H.; Shin, J.H.; Soutter, H.H.; Strohbach, J.W.; Symanowicz, P.T.; Thomason, J.R.; Trzupek, J.D.; Vargas, R.; Vincent, F.; Yan, J.; Zapf, C.W.; Wright, S.W. Discovery of Clinical Candidate 1-{[(2S,3S,4S)-3-Ethyl-4-fluoro-5-oxopyrrolidin-2-yl]methoxy}-7-methoxyisoquinoline-6-carboxamide (PF-06650833), a Potent, Selective Inhibitor of Interleukin-1 Receptor Associated Kinase 4 (IRAK4), by Fragment-Based Drug Design. *J. Med. Chem.* **2017**, *60*, 5521-5542, https://doi.org/10.1021/acs.jmedchem.7b00231.
21. Halgren, T.A. Merck molecular force field. I. Basis, form, scope, parameterization, and performance of MMFF94. *J. Comput. Chem.* **1998**, *17*, 490-519, https://doi.org/10.1002/(SICI)1096-987X(199604)17:5/6%3C490::AID-JCC1%3E3.0.CO;2-P.
22. Morris, G.M.; Goodsell, D.S.; Halliday, R.S.; Huey, R.; Hart, W.E.; Belew, R.K.; Olson, A.J. Automated docking using a Lamarckian genetic algorithm and an empirical binding free energy function. *J. Comput. Chem.* **1998**, *19*, 1639-1662, https://doi.org/10.1002/(SICI)1096-987X(19981115)19:14%3C1639::AID-JCC10%3E3.0.CO;2-B.
23. Solis, F.J.; Wets, R.J.-B. Minimization by Random Search Techniques. *is Math. Oper. Res.* **1981**, *6*, 19-30, https://doi.org/10.1287/moor.6.1.19.
24. Mujtaba, M.; Shafiq, M.I.; Ahmad, A.; Al-Otaibi, J.S.; Daglia, M.; Khan, H. Halogenated Curcumin Derivatives: SwissADME/ADMT, DFT and Biological Targets Prediction. *Chem. Afr.* **2025**, *8*, 5499-5515, https://doi.org/10.1007/s42250-025-01452-4.
25. Al Azzam, K.M. SwissADME and pkCSM Webservers Predictors: an integrated Online Platform for Accurate and Comprehensive Predictions for In SilicoADME/T Properties of Artemisinin and its Derivatives. *Kompl. Ispolz. Min. Syra* **2023**, *325*, 14-21, https://doi.org/10.31643/2023/6445.13.
26. Askerova, U.F. PREDICTION OF ACUTE TOXICITY FOR (Z)-3-(2-PHENYLHYDRAZINYLIDENE)BENZOFURAN-2(3H)-ONE AND ITS DERIVATIVES FOR RATS USING GUSAR PROGRAM. *New Mater. Compd. Appl.* **2023**, *7*, 50-56.
27. McElroy, W.T. Interleukin-1 receptor-associated kinase 4 (IRAK4) inhibitors: an updated patent review (2016-2018). *Expert Opin. Ther. Pat.* **2019**, *29*, 243-259, https://doi.org/10.1080/13543776.2019.1597850.

28. Shrivastava, D.; Gupta, L.K.; Yerrapureddy, A.R.; Nune, S.S.K. Synthesis and *in vitro* characterization of novel IRAK-4 inhibitor compounds. *Prep. Biochem. Biotechnol.* **2026**, 1-17, https://doi.org/10.1080/10826068.2026.2620804.
29. Khanfar, M.A.; Alqtaishat, S. Discovery of potent IRAK-4 inhibitors as potential anti-inflammatory and anticancer agents using structure-based exploration of IRAK-4 pharmacophoric space coupled with QSAR analyses. *Comput. Biol. Chem.* **2019**, *79*, 147-154, https://doi.org/10.1016/j.compbiolchem.2019.02.005.
30. Zhao, Y.; Wan, Q.; He, X. Construction of IRAK4 inhibitor activity prediction model based on machine learning. *Mol. Divers.* **2024**, *28*, 2289-2300, https://doi.org/10.1007/s11030-024-10926-5.
31. Xiang, F. Therapeutic compounds targeting interleukin-1 receptor-associated kinase 4 (IRAK4): an updated patent review (2019 to present). *Expert Opin. Ther. Pat.* **2024**, *34*, 1137-1166, https://doi.org/10.1080/13543776.2024.2406825.
32. Bugnon, M.; Röhrig, U.F.; Goullieux, M.; Perez, M.A.S.; Daina, A.; Michielin, O.; Zoete, V. SwissDock 2024: major enhancements for small-molecule docking with Attracting Cavities and AutoDock Vina. *Nucleic Acids Research* **2024**, *52*, W324-W332, https://doi.org/10.1093/nar/gkae300.
33. Guedes, I.A.; Pereira da Silva, M.M.; Galheigo, M.; Krempser, E.; de Magalhães, C.S.; Correa Barbosa, H.J.; Dardenne, L.E. DockThor-VS: A Free Platform for Receptor-Ligand Virtual Screening. *J. Mol. Biol.* **2024**, *436*, 168548, https://doi.org/10.1016/j.jmb.2024.168548.
34. Alhusayni, A.A. The Role of AutoDock and Related Techniques in Bioinformatics for Developing Immune Proteins and Therapeutic Treatments. *Infinity Med. Innov.* **2025**, *1*, 62-66.
35. Friesner, R.A.; Murphy, R.B.; Zhang, Y.; Xiong, Y.; Devlaminck, P.A.; Tubert-Brohman, I.; Jerome, S.V. Glide WS: Methodology and Initial Assessment of Performance for Docking Accuracy and Virtual Screening. *J. Chem. Theory Comput.* **2025**, *21*, 12696-12708, https://doi.org/10.1021/acs.jctc.5c01316.
36. Muhammed, M.; Aki-Yalcin, E. Molecular docking: principles, advances, and its applications in drug discovery. *Letters in Drug Design & Discovery*, **2024**, 21(3), 480-495. . https://doi.org/10.2174/1570180819666220922103109
37. Wu, Q.; Huang, S.-Y. XDock: A General Docking Method for Modeling Protein–Ligand and Nucleic Acid–Ligand Interactions. *J. Chem. Inf. Model.* **2024**, *64*, 9563-9575, https://doi.org/10.1021/acs.jcim.4c00855.
38. Figueroa-Valverde, L.; Díaz-Cedillo, F.; Rosas-Nexticapa, M.; Alvarez-Ramirez, M.; Mateu-Armad, M.V.; López-Ramos, M.; López-Gutierrez, T. Interaction of some amino-nitrile derivatives with vascular endothelial growth factor receptor 1 (VEGFR1) using a theoretical model. *Drug Res.* **2023**, *73*, 355-364, https://doi.org/10.1055/a-2062-3571.
39. Almajidi, Y.Q.; Faisal, R.R.; Yaseen, A. GastroPlus® as simulating/conducting software for modeling physiologically-based pharmacokinetics & physiologically based biopharmaceutics. *Maaen J. Med. Sci.* **2025**, *4*, 10, https://doi.org/10.55810/2789-9136.1078.
40. Gutierrez, L.; Hernández, M.; Del Villar, J.L.; Sánchez, Z.; Sumano, H. Pharmacokinetic evaluation of a long-acting, tasteless oral formulation of enrofloxacin in dogs. *Open Vet. J.* **2025**, *15*, 5009, https://doi.org/10.5455/OVJ.2025.v15.i10.19.
41. Yu, B.; Mei, K.; Zhan, D.; Tang, Q.; Cai, H.; Zhang, R. Establishment of a Vancomycin Population Pharmacokinetic Model for Pediatric Patients Based on the Non-Linear Mixed-Effects Model. *Drugs R&D* **2025**, *25*, 309-320, https://doi.org/10.1007/s40268-025-00523-8.
42. Li, Y.; Sun, H.; Zhang, Z. The Evolution and Future Directions of PBPK Modeling in FDA Regulatory Review. *Pharmaceutics* **2025**, *17*, 1413, https://doi.org/10.3390/pharmaceutics17111413.
43. Bakchi, B.; Krishna, A.D.; Sreecharan, E.; Ganesh, V.B.J.; Niharika, M.; Maharshi, S.; Puttagunta, S.B.; Sigalapalli, D.K.; Bhandare, R.R.; Shaik, A.B. An overview on applications of SwissADME web tool in the design and development of anticancer, antitubercular and antimicrobial agents: A medicinal chemist's perspective. *J. Mol. Struct.* **2022**, *1259*, 132712, https://doi.org/10.1016/j.molstruc.2022.132712.
44. Hua, Z.L. Elucidating the Role of Cytochrome p450 Enzymes in Drug Metabolism and Interactions. *Clin. J. Med. Health Pharm.* **2024**, *2*, 1-10.
45. Laaboub, N.; Vandenberghe, F.; Ansermot, N.; Piras, M.; Ranjbar, S.; Petrovic, D.; Pistis, G.; Vandenberghe-Dürr, S.; Strippoli, M.-P.F.; Marques-Vidal, P.; Ponte, B.; Pruijm, M.; Vogt, B.; Gamma, F.; von Gunten, A.; Plessen, K.J.; Conus, P.; Crettol, S.; Vollenweider, P.; Preisig, M.; Bochud, M.; Eap, C.B. Dietary caffeine to assess CYP1A2 activity, tailor clozapine doses, and predict treatment response: genetic, epigenetic and clinical analyses. *Mol. Psychiatry* **2026**, *31*, 1420-1430, https://doi.org/10.1038/s41380-025-03256-x.

46. Tu, D.-Z.; Liu, P.-Q.; Zhu, G.-H.; Zeng, H.-R.; Deng, Y.-Y.; Huang, J.; Niu, X.-T.; Liu, Y.-F.; Hu, J.; Liang, X.-M.; Finel, M.; Wang, P.; Ge, G.-B. Human UDP-glucuronosyltransferase 1As catalyze aristolochic acid D O-glucuronidation to form a lesser nephrotoxic glucuronide. *J. Ethnopharmacol.* **2024**, *328*, 118116, https://doi.org/10.1016/j.jep.2024.118116.
47. Kim, D.; Ahn, S.; Choi, J. Identification of developmental and reproductive toxicity of biocides in consumer products using ToxCast bioassays data and machine learning models. *Environ. Int.* **2025**, *202*, 109621, https://doi.org/10.1016/j.envint.**2025**.109621.
48. Ortiz-Andrade, R.; Araujo-León, J.A.; Sánchez-Recillas, A.; Navarrete-Vazquez, G.; González-Sánchez, A.A.; Hidalgo-Figueroa, S.; Alonso-Castro, Á.J.; Aranda-González, I.; Hernández-Núñez, E.; Coral-Martínez, T.I.; Sánchez-Salgado, J.C.; Yáñez-Pérez, V.; Lucio-Garcia, M.A. Toxicological Screening of Four Bioactive Citroflavonoids: In Vitro, In Vivo, and In Silico Approaches. *Molecules* **2020**, *25*, 5959, https://doi.org/10.3390/molecules25245959.
49. Mendes da Silva, L.; Andrade–Vieira, L.F. Ecotoxicological bioassays with terrestrial plants: a holistic view of standards, guidelines, and protocols. *J. Toxicol. Environ. Health B Crit. Rev.* **2025**, *28*, 183-221, https://doi.org/10.1080/10937404.2024.2440876.
50. Srivastava, R. Theoretical Studies on the Molecular Properties, Toxicity, and Biological Efficacy of 21 New Chemical Entities. *ACS Omega* **2021**, *6*, 24891-24901, https://doi.org/10.1021/acsomega.1c03736.
51. Lagunin, A.; Lisitsa, E.; Rudik, A.; Ivanov, S.; Dmitriev, A.; Muraviova, E.; Poroikov, V. QSAR Modeling for Predicting IC50 and GI50 Values for Human Cell Lines Used in Toxicological Studies. *Int. J. Mol. Sci*. **2025**, *26*(24), 12063.
52. Pouretedal, H.R.; Keshavarz, M.H.; Abbasi, A. A new approach for accurate prediction of toxicity of amino compounds. *J. Iran. Chem. Soc.* **2015**, *12*, 487-502, https://doi.org/10.1007/s13738-014-0506-7.

Publisher's Note & Disclaimer